PERGAMON

International Journal of Solids and Structures 39 (2002) 5465–5479

INTERNATIONAL JOURNAL OF SOLIDS and STRUCTURES

www.elsevier.com/locate/ijsolstr

Acoustic emission from strain-determined sources

Franz Ziegler *

Technical University of Vienna, Wiedner-Hauptstrasse 8-10 / E201, A-1040 Vienna, Austria

Received 17 October 2001; received in revised form 26 February 2002

Abstract

Monitoring of structures can be based on observing signals emitted in the course of developing defects. Layered ductile structures are considered which react on overloads by the formation of (small scale) plastic zones. Within the linear elastic background concept such an event is considered by the formation of sources of eigenstress. Since a direct description of the source characteristics is rather cumbersome, alternatively, the time convolution of the imposed plastic strains with the complementary Green's stress dyadic is proposed to describe the signal of the acoustic emission. Thus, the dynamic generalization of Maysel's formula of thermo-elasticity, a special form of the dynamic reciprocity theorem, enters the field of computational "nondestructive evaluation". In that context, the novel contribution of this paper to acoustic emission and monitoring of structures is the formulation of the full three-dimensional problems and, for layered structures, the construction of the generalized rays (plane wave expansions) in the background, considering an instantaneous oblique force point source at the transducer's location. Consequently, all information on the wave guide is contained in the Green's stress dyadic. The Laplace transformed solution is worked out for localized plastic sources. Deconvolution and transducer dynamics is not discussed here.

Keywords: Wave fields; Plastic sources; Green's function; Layered composites

1. Introduction

Professor Jan D. Achenbach made fundamental contributions to quantitative ultrasonics and nondestructive evaluation, see e.g. Achenbach et al. (1982, 1987). In that connection he applied the dynamic reciprocity theorem for analyzing scattering and also diffraction, which, in a special setting, is crucial in reformulating the acoustic emission problem as shown in this paper.

Commonly, acoustic emission stands for the technology that has been developed to locate and to determine the characteristics of a source which emits elastic waves. In its application to materials characterization, the sources may be point defects in crystals, grain boundary movement of polycrystallines, including the phenomenon of twinning, creation and collapsing of voids, etc., see Simmons and Wadley (1984) for a theoretical account and further relevant references. Moreover, acoustic emission has become a

* Tel.: +43-1-58801-201-10; fax: +43-1-58801-201-99.
E-mail address: franz.ziegler@tuwien.ac.at (F. Ziegler).

0020-7683/02/$ - see front matter
PII: S0020-7683(02)00359-1

major technique for continuously monitoring the integrity of high risk structures. In this connection, the sources of principal interest are plastic deformation, which is the contents of this paper, and crack growth as well (Mal, 2001). Guo et al. (1996) studied the characteristics of guided waves generated by crack initiation in thin composite laminates. Geophysical investigations to measure microseismic activity are highly developed for applications in rock mechanics, see also Aki and Richards (1980, ch. 3).

The common theoretical foundation of acoustic emission contains basic theories for detecting the source location (by triangulation), describing the source mechanism, the signal dispersion and, finally, the kinetic and kinematic source characterization (by deconvolution and other semi-inverse procedures). Pao (1978), dealt with all these aspects by applying the classical Green's function approach, see also the exhaustive list of references given there, with further progress reviewed in Pao et al. (1984). Modeling the source by double forces in a plate, a detailed study was made by Ceranoglu and Pao (1981)—with the experimental results and the transducer dynamics included in the analysis by Sachse (1987). A detailed study was made by Ohira and Pao (1987).

This paper is mainly concerned with the aspect of signal dispersion and presents a complementary Green's function approach. Thus, it is shown that it is possible to avoid several of the complications which are necessarily associated with the classical approach. In order to illustrate this novel analysis, plastic sources are considered in rods (under the approximating condition of one-dimensional stress) and subsequently in three-dimensional bodies. Thereby, it becomes obvious to expand the Green's function of the second kind in question into plane waves for the case of layered wave guides with plane interfaces. Thus, the theory of generalized ray integrals is rendered applicable for the waves emitted from localized sources which can be characterized by imposed strains, like plastic sources. Use of the background concept is crucial, see also Irschik and Ziegler (1995) for uniaxial elastic–plastic stress waves, Fotiu et al. (1991) for the background concept, and, for elastic–plastic spherical waves with point symmetry, Fotiu and Ziegler (1996). The background is defined by the elastic wave guide without imposed strains, thus, in this sense, the procedure makes use of the multiple field approach.

2. Internal sources in thin rods

To illustrate the background concept, a plastic source is considered uniformly distributed over the cross sectional area A in a semi-infinite rod. A plastic strain increment $\overline{\Delta\varepsilon}$ emits stress waves propagating with the sound speed $c = \sqrt{E/\rho}$ in the background rod, as shown in the Mach-plane in Fig. 1. Reflection at the free end, $x = 0$, is indicated. Based on the generalized rate form of Hooke's law in uni-axial stress, the non-homogeneous wave equation for the axial displacement u results from conservation of momentum,

$$\dot{\sigma} = E\left(\dot{\varepsilon} - \dot{\bar{\varepsilon}}\right), \quad u_{,xx} - c^{-2}u_{,tt} = \bar{\varepsilon}_{,x}, \quad c^2 = E/\rho \tag{1}$$

The elastic–viscoplastic waves resulting from overloads have been calculated by incremental superposition of the elastic waves in the background by Irschik and Ziegler (1990) and, for the more general setting, see Irschik and Ziegler (1995).

Classically, the direct Green's function approach to Eq. (1) considers a singular internal source,

$$\bar{\varepsilon}_{,x} = \delta_{,x}(x - \xi)\delta(t - \tau) \tag{2}$$

and presents the solution for distributed sources in terms of Green's displacement $\tilde{u}(x, \xi; t)$ of the infinite rod. Consequently, boundary conditions and the waves created by reflection must be considered separately, see again Fig. 1.

Alternatively, the complementary approach considers the force Green's function $\tilde{\sigma}(\xi, x; t)$ of the background wave guide, thus, including surface effects. However, the buried unit instantaneous force $F(t)$ is

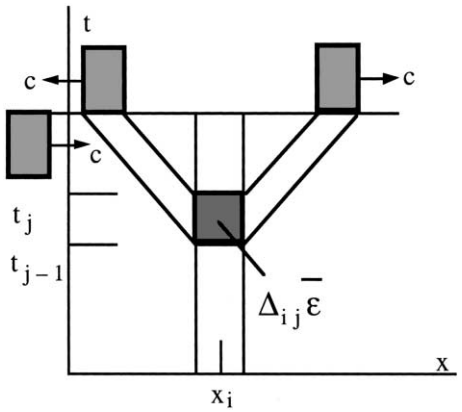

Fig. 1. Acoustic emission from a local plastic source in a semi-infinite rod, stress wave in Mach-plane shown. Transducer in receiving mode at $x = 0$, during monitoring of the rod.

applied in the point of observation x and, integration is performed over the distributed source points. Time convolution with the plastic strain is common to both integral representations. In the time Laplace transform domain, the particular solution of Eq. (1) takes on the form of the dynamic Maysel's formula, for its thermoelastic origin, see e.g., Ziegler (1998, ch. 6),

$$u(x,s) = \int_0^l \tilde{\sigma}(\xi,x;s)\bar{\varepsilon}(\xi,s)A\,\mathrm{d}\xi, \tag{3}$$

For the infinitely long rod, note the reciprocity, $\tilde{\sigma}(\xi,x,s) = \tilde{u}(x,\xi;s)$ where, ε is the direction factor,

$$\tilde{\sigma}(\xi,x,s) = -\frac{\varepsilon}{2}\frac{F(s)}{A}\exp\frac{s}{c}|\xi - x|, \quad \varepsilon = \pm 1$$

When monitoring such a rod with respect to the development of plastic strain, the displacement $u(x = 0;t)$ is received by a transducer placed at the free end, see Fig. 2. Hence, the complementary Green's function of the second kind that is produced by the singular surface traction enters Eq. (3). Performing the limit $x \to 0$ in Eq. (3), i.e. considering the reflection, yields,

$$\tilde{\sigma}(\xi,s) = -\frac{F(s)}{A}\exp -\frac{s}{c}\xi. \tag{4}$$

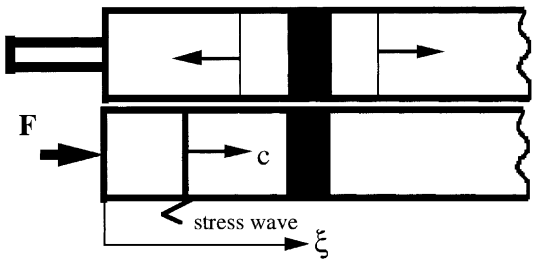

Fig. 2. Monitoring an elastic–plastic rod with a transducer in receiving mode attached. Since the point of observation is on the surface, we substitute the surface load, i.e. Green's function of the second kind, Eq. (4), in Eq. (3).

If the signal emitted from a sufficiently isolated buried plastic source (see again Fig. 1) needs to be observed, the spatial integration in Eq. (3) can be approximated say by the rectangular rule, while Eq. (4) is being substituted. The transducer dynamics is not included in Eq. (3) which solely renders the free field solution. Deconvolution is not within the scope of this paper.

3. Acoustic emission from a plastic point source

In this section, the three-dimensional plastic source, localized in a small volume, is considered with respect to acoustic emission and, by domain integration, the extension to a plastic zone is performed. Consequently, in the classical approach, the particular solution of the nonhomogeneous wave equations resulting in the infinite background domain is given in terms of the direct Green's function by the domain and convolution integrals, see e.g. Eringen and Suhubi (1975), for the displacement in a direction i,

$$u_i(\boldsymbol{x},t)=\int_0^t \mathrm{d}\tau \int_V \tilde{\boldsymbol{u}}_{i(\alpha\beta)}(\boldsymbol{x},\boldsymbol{x}_0;t-\tau)\overline{\varepsilon_{\alpha\beta}}(\boldsymbol{x}_0,\tau)\,\mathrm{d}V(\boldsymbol{x}_0). \tag{5}$$

Eq. (5) is the basis of analysis of acoustic emission from material phase transformations, see e.g. Simmons and Wadley (1984). Analogously, Pao (1978), applied the Green's displacement dyadic to derive solutions for dynamic nuclei of strains (see the list of papers in acoustic emission there). As a serious drawback, complicating surface integrals have to be considered for finite domains, for the simple case of reflection at the free end of a rod, see again Fig. 1.

Yet, the generalized dynamic Maysel's formula (originally stemming from thermoelasticity) displays a more promising characteristic. As for the three-dimensional case it has already been derived by Irschik et al. (1993), for the uniaxial case see again Eq. (3), and for the point symmetrical case see Fotiu and Ziegler (1996). On the one hand Maysel's formula contains also time convolution, but on the other hand it is complementary to Eq. (5) with respect to the spatial integration. Therefore, the dynamic force creating the Green's function is applied at the point of observation (at the location of the transducer) and, above all, it holds good for those finite bodies with boundary conditions given in the form of prescribed displacements on parts of the surface while the remaining surface parts are kept free of traction. If the b.c. both of the original problem (with plastic sources) and the background structure (with instantaneous force load) are identical, the contribution of the surface integral (the work of traction) vanishes.

Considering the more general case where nonhomogeneous initial conditions are prescribed in a time stepping procedure, an additional domain integral needs to be added to Maysel's formula. The particular solution in the Laplace transform domain, with the observational point at $\boldsymbol{x}_0$, is as follows:

$$u_i(\boldsymbol{x}_0;s)=\int_V \tilde{\boldsymbol{\sigma}}_{\alpha\beta(i)}(\boldsymbol{x},\boldsymbol{x}_0;s)\bar{\varepsilon}_{\alpha\beta}(\boldsymbol{x};s)\,\mathrm{d}V(\boldsymbol{x})+\rho\int_V\left[\dot{\tilde{\boldsymbol{u}}}_{\alpha(i)}(\boldsymbol{x},\boldsymbol{x}_0;s)\bar{\boldsymbol{u}}_{\alpha 0}(\boldsymbol{x})+\tilde{\boldsymbol{u}}_{\alpha(i)}(\boldsymbol{x},\boldsymbol{x}_0;s)\dot{\bar{\boldsymbol{u}}}_{\alpha 0}(\boldsymbol{x})\right]\mathrm{d}V(\boldsymbol{x}) \tag{6}$$

Note the change of coordinate notation when comparing Eqs. (6) and (3) and apply the summation convention. Acoustic emission of a single plastic event is merely given by the convolution contained in the first line of Eq. (6). In such a case, the remaining volume integral of Maysel's formula can be approximated by the rectangular rule of numerical integration, which means by multiplying the integrand with the cell-volume of the concentrated plastic source. The point of observation $\boldsymbol{x}_0$ is commonly placed on the surface with a transducer in receiving mode attached.

Eq. (6) becomes a fine working tool for monitoring layered structures with plane interfaces since then the Green's dyadic can be expanded into plane waves and the whole information of the wave guide is contained in the generalized ray integrals.

Note in the case of infinite bodies the reciprocity of the influence functions of stress and displacement in the Eqs. (5) and (6), which has been already mentioned with respect to Eq. (3) for the uniaxial stress state of the infinite rod,

$$\tilde{\boldsymbol{\sigma}}_{\alpha\beta(i)}(\boldsymbol{x},\boldsymbol{x}_0;s)=\tilde{\boldsymbol{u}}_{i(\alpha\beta)}(\boldsymbol{x}_0,\boldsymbol{x};s) \tag{7}$$

3.1. The three-dimensional dynamic Green functions expanded in plane waves

Consequently, acoustic emission from a concentrated plastic source (in a single cell) should be observed primarily in Eq. (6). However, the influence functions must be presented in a suitable form for inversion of the Laplace transform and for taking into account reflections on the traction free surface of a half space, at the interface of a surface layer, at the surfaces of a plate or wedge-shaped wave guide, etc. The expansion into plane waves, i.e. the resulting generalized ray theory, seems appropriate for short observation times, see also Ziegler and Borejko (2000). Subsequently, we suppress the tilde indicating the Green's function in the background.

3.1.1. Basic equations of elastic body waves

To keep the paper self-contained, we note the Helmholtz decomposition of the displacements in a homogeneous and isotropic linear elastic solid. It yields the set of wave equations for P- and S-waves, in absence of body forces, see Achenbach (1973),

$$\boldsymbol{u}=\operatorname{grad}\phi+\operatorname{curl}\boldsymbol{\psi},\quad \Delta\phi=c^{-2}\ddot{\phi},\quad \Delta\boldsymbol{\psi}=C^{-2}\ddot{\boldsymbol{\psi}},\quad \operatorname{div}\boldsymbol{\psi}=0 \tag{8}$$

Furthermore the three components of stresses, given by Hooke's law, enter the "internal" boundary value problems of vertical and horizontal single forces to be considered below

$$\sigma_{zz}=\lambda c^{-2}\ddot{\phi}+2\mu\left(\frac{\partial^2\phi}{\partial z^2}+\frac{\partial^2\psi_y}{\partial x\,\partial z}-\frac{\partial^2\psi_x}{\partial y\,\partial z}\right),\quad \sigma_{zx}=\mu\left[-C^{-2}\ddot{\psi}_y+2\left(\frac{\partial^2\phi}{\partial x\,\partial z}-\frac{\partial^2\psi_x}{\partial x\,\partial y}+\frac{\partial^2\psi_y}{\partial x^2}\right)\right],$$
$$\sigma_{zy}=\mu\left[-C^{-2}\ddot{\psi}_x+2\left(\frac{\partial^2\phi}{\partial y\,\partial z}-\frac{\partial^2\psi_z}{\partial x\,\partial z}+\frac{\partial^2\psi_x}{\partial z^2}\right)\right]. \tag{9}$$

where $c^2=(\lambda+2\mu)/\rho$ and $C^2=\mu/\rho$ are the squared body wave speeds of P- and S-waves, respectively.

3.1.2. Vertical instant single force

Laplace-transformation in time, Fourier transformations with respect to the horizontal (x,y) coordinates, render the solution via the three conditions provided by the internal b.v. problem

$$z=0:\tilde{\bar{\boldsymbol{\sigma}}}_{zz}(\xi,\kappa,x)=-\frac{1}{2}\varepsilon_z\underline{Q}_z\bar{\boldsymbol{f}}(s),\quad u_x=u_y=0 \tag{10}$$

Thus, the body wave potentials are yielded by the Weyl–Sommerfeld integrals, which means they are expanded into plane waves. For detailed derivations see Pao and Gajewski (1977), Borejko and Ziegler (1998, 2002). The following Eq. (11) summarizes the Laplace transformed results with the important phase–time relationship indicated, which is crucial for the determination of the arrival times, axial symmetry is apparent but not built-in,

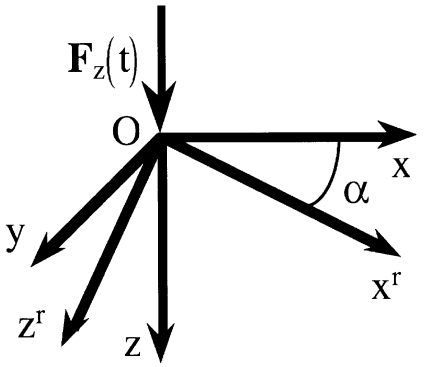

Fig. 3. Vertical force in infinite space. Rotation of coordinates about the y-axis indicated.

$$
\begin{aligned}
&\overline{\phi^z}(x,y,z,s) = s^2 Q_z \overline{F}(s) \int_{-\infty}^{\infty}\int_{-\infty}^{\infty} S_P^z \exp(s g_P)\,\mathrm{d}\xi\,\mathrm{d}\kappa,\\
&-t = g_P = \mathrm{i}\xi x + \mathrm{i}\kappa y - \eta|z - z_0|, \quad \eta = \sqrt{c^{-2} + \xi^2 + \kappa^2},\\
&\bar{\psi}_j^z(x,y,z,s) = s^2 Q_z \overline{F}(s) \int_{-\infty}^{\infty}\int_{-\infty}^{\infty} S_{Sj}^z \exp(s g_S)\,\mathrm{d}\xi\,\mathrm{d}\kappa,\\
&-t = g_S = \mathrm{i}\xi x + \mathrm{i}\kappa y - \zeta|z - z_0|, \quad \zeta = \sqrt{C^{-2} + \xi^2 + \kappa^2}, \quad j = x, y\\
&\bar{\psi}_z^z(x,y,z,s) = 0,\\
&\overline{F}(s) = \bar{f}(s)/8\pi^2 s^2 \rho, \quad S_P^z = -\varepsilon_z, \quad S_{Sx}^z = -\frac{\mathrm{i}\kappa}{\zeta}, \quad S_{Sy}^z = \frac{\mathrm{i}\xi}{\zeta}
\end{aligned}
\tag{11}
$$

The direction factor ε_z takes on the value $+1$ for a downward propagating ray, $z - z_0 > 0$, and is set -1 for $z - z_0 < 0$, for an upward propagating plane wave.

The wave potentials, e.g. those specialized for a vertical force given in Eq. (11), can be easily transformed into rotated coordinates (see Fig. 3) by enforcing the following invariance conditions for the plane wave amplitudes and phases, where Eq. (12) holds for P- and S-waves, respectively,

$$
\begin{aligned}
&S\,\mathrm{d}\xi\,\mathrm{d}\kappa = S^r\,\mathrm{d}\xi^r\,\mathrm{d}\kappa, \quad -t = g = g^r = \mathrm{i}\xi x + \mathrm{i}\kappa y - (\eta,\zeta)|z| = \mathrm{i}\xi^r x^r + \mathrm{i}\kappa y - (\eta,\zeta)^r|z^r|\\
&\mathrm{i}\xi^r = \mathrm{i}\xi\cos\alpha - (\eta,\zeta)\sin\alpha, \quad \mathrm{i}\kappa^r = \mathrm{i}\kappa
\end{aligned}
\tag{12}
$$

Thus, in general, Eq. (12) allows us to classically consider the reflection of the source ray at an inclined interface, say of a wedge type surface layer. See also Section 3.3 for the limiting process to be performed for an interlayer plastic source. The axisymmetric waves in an elastic layer are studied by Achenbach (2000) using elastodynamic reciprocity. The latter is related to the dynamic Maysel's formula, Eq. (6).

3.1.3. Horizontal instant single forces

The instantaneous forces are considered to act in the x- and y-directions, respectively, and the internal b.v. problems yield alternated emittance functions as listed in Table 1,

$$
\begin{aligned}
&z = 0 : \tilde{\bar{\sigma}}_{zx}(\xi,\kappa,s) = -\tfrac{1}{2}\varepsilon_z Q_x \bar{f}(s), \quad u_z = u_y = 0\\
&z = 0 : \tilde{\bar{\sigma}}_{zy}(\xi,\kappa,s) = -\tfrac{1}{2}\varepsilon_z Q_y \bar{f}(s), \quad u_z = u_x = 0
\end{aligned}
\tag{13}
$$

The following displacement potentials hold good for horizontal forces applied in the x- and y-directions, respectively, by putting alternatively $j = x, y$,

Table 1
Emittance functions of horizontal forces

$S_P^x = C^{-2}\frac{\mathrm{i}\xi}{\eta}\frac{\eta}{\Delta_x}$,	$S_{Sx}^x = \varepsilon_z\xi\kappa\frac{\eta-\zeta}{\Delta_x}$,	$S_{Sy}^x = \varepsilon_z$
$S_{Sz}^x = \mathrm{i}\kappa\frac{\eta\zeta-\xi^2-\kappa^2}{\Delta_x}$,	$\Delta_x = \eta(\zeta^2-\xi^2)-\zeta\kappa^2$	
$S_P^y = C^{-2}\frac{\mathrm{i}\kappa}{\eta}\frac{\eta}{\Delta_y}$,	$S_{Sx}^y = -\varepsilon_z, S_{Sy}^y = -\varepsilon_z\xi\kappa\frac{\eta-\zeta}{\Delta_y}$	
$S_{Sz}^y = -\mathrm{i}\xi\frac{\eta\zeta-\xi^2-\kappa^2}{\Delta_y}$,	$\Delta_y = \eta(\zeta^2-\kappa^2)-\zeta\xi^2$	

$$\overline{\phi^j}(x,y,z,s) = s^2 Q_j \overline{F}(s)\int_{-\infty}^{\infty}\int_{-\infty}^{\infty} S_P^j \exp(sg_P)\,\mathrm{d}\xi\,\mathrm{d}\kappa \tag{14}$$

$$\begin{aligned}
\bar{\psi}_x^j(x,y,z,s) &= s^2 Q_j \overline{F}(s)\int_{-\infty}^{\infty}\int_{-\infty}^{\infty} S_{Sx}^j \exp(sg_S)\,\mathrm{d}\xi\,\mathrm{d}\kappa\\
\bar{\psi}_y^j(x,y,z,s) &= s^2 Q_j \overline{F}(s)\int_{-\infty}^{\infty}\int_{-\infty}^{\infty} S_{Sy}^j \exp(sg_S)\,\mathrm{d}\xi\,\mathrm{d}\kappa\\
\bar{\psi}_z^j(x,y,z,s) &= s^2 Q_j \overline{F}(s)\int_{-\infty}^{\infty}\int_{-\infty}^{\infty} S_{Sz}^j \exp(sg_S)\,\mathrm{d}\xi\,\mathrm{d}\kappa
\end{aligned} \tag{15}$$

The emittance functions listed in Table 1 are to be substituted.

Hence, comparing Eqs. (14) and (15) with Eq. (11) the following striking differences are to be recognized:

(i) The vector potentials in case of horizontal forces have three nonvanishing components.
(ii) The emittance functions in case of horizontal forces, which need to be substituted into Eqs. (14) and (15) are listed in Table 1. They are totally coupled due to the characteristic determinants Δ_x, Δ_y of the linear equations resulting from the internal b.v. problem, Eq. (13).
(iii) Axial symmetry is no longer apparent.

3.1.4. The oblique force

The still buried oblique force can be decomposed into its Cartesian components. Hence, it is possible to arrive at the desired solution of the generated body waves by superposition of the wave potentials given in Section 3.1.2 for the vertical component and in Section 3.1.3 for the horizontal components, with a common time source function (Laplace transformed $\overline{F}(s)$) understood, as follows:

$$\overline{\phi}(x,y,z,s) = s^2\overline{F}(s)\int_{-\infty}^{\infty}\int_{-\infty}^{\infty} S_P \exp(sg_P)\,\mathrm{d}\xi\,\mathrm{d}\kappa,\quad S_P = Q_x\frac{\mathrm{i}\xi}{C^2\Delta_x} - Q_y\frac{\mathrm{i}\kappa}{C^2\Delta_y} - Q_z\varepsilon_z; \tag{16}$$

$$\begin{aligned}
\bar{\psi}_x &= s^2\overline{F}(s)\int_{-\infty}^{\infty}\int_{-\infty}^{\infty} S_{Sx}\exp(sg_S)\,\mathrm{d}\xi\,\mathrm{d}\kappa,\quad S_{Sx} = Q_x\frac{\varepsilon_z\xi\kappa(\eta-\zeta)}{\Delta_x} - Q_y\varepsilon_z - Q_z\frac{\mathrm{i}\kappa}{\zeta};\\
\bar{\psi}_y &= s^2\overline{F}(s)\int_{-\infty}^{\infty}\int_{-\infty}^{\infty} S_{Sy}\exp(sg_S)\,\mathrm{d}\xi\,\mathrm{d}\kappa,\quad S_{Sy} = Q_x\varepsilon_z - Q_y\frac{\varepsilon_z\xi\kappa(\eta-\zeta)}{\Delta_y} + Q_z\frac{\mathrm{i}\xi}{\zeta};\\
\bar{\psi}_z &= s^2\overline{F}(s)\int_{-\infty}^{\infty}\int_{-\infty}^{\infty} S_{Sz}\exp(sg_S)\,\mathrm{d}\xi\,\mathrm{d}\kappa,\quad S_{Sz} = [\eta\zeta-(\xi^2+\kappa^2)]\left[Q_x\frac{\mathrm{i}\kappa}{\Delta_x} - Q_y\frac{\mathrm{i}\xi}{\Delta_y}\right].
\end{aligned} \tag{17}$$

For time-harmonic waves in an elastic layer, see Achenbach and Xu (1999). Thus it becomes obvious above that the summation of potential functions is solely executed in the various resulting emittance functions S.

3.2. The three-dimensional complementary dynamic Green functions of the second kind expanded in plane waves, oblique force on the surface of a half-space

Considering a transducer in the receiving mode at the traction free surface requires to put the instantaneous force at this location. Therefore, in order to construct a limiting process, two steps are necessary. Firstly, the buried force and a deeper down located receiver are considered in the infinite body. The wave potentials, denoted by a subscript zero in Eqs. (18) and (19) are given by Eqs. (16) and (17) with direction factor $\varepsilon_z = +1$ substituted, see also the phase functions in Eq. (11) where $z - z_0 > 0$. Secondly, the potentials of the waves reflected at the free surface of the half space to be considered here, are to be superposed. For instance, the reflection of the incident P-wave (first segment pointing upwards, direction factor $\varepsilon_z = -1$ in Eq. (16)) yields the *Pp* and *Ps* reflected rays. Analogously, reflection of the incident S-wave is considered, for details see e.g. Pao and Gajewski (1977), Borejko and Ziegler (2002).

The limiting process $z_0 \to 0$ is subsequently performed as indicated below and yields the emittance functions in the wave potentials of the oblique surface force,

$$\overline{\varphi_p} = \overline{\phi_0} + \lim_{z_0 \to 0} \left(\overline{\varphi_{Pp}} + \sum_k \overline{\varphi_{S,kp}} \right), \quad S_p = S_{0p} + S_P R^{PP} + \sum_k S_{S,k} R^{S,kP}, \quad k = x, y, z;$$

or explicitly,

$$\begin{aligned} S_p = {} & Q_x \left[(1 + R^{PP}) \frac{\mathrm{i}\xi}{C^2 \Delta_x} - R^{S_x P} \frac{\xi\kappa(\eta - \zeta)}{\Delta_x} - R^{S_y P} \right] + Q_y \left[-(1 + R^{PP}) \frac{\mathrm{i}\kappa}{C^2 \Delta_y} + R^{S_x P} + R^{S_y P} \frac{\xi\kappa(\eta - \zeta)}{\Delta_y} \right] \\ & + Q_z \left[(-1 + R^{PP}) - R^{S_x P} \frac{\mathrm{i}\kappa}{\zeta} + R^{S_y P} \frac{\mathrm{i}\xi}{\zeta} \right] \end{aligned}$$

$$\overline{\varphi_p} = s^2 \overline{F}(s) \int_{-\infty}^{\infty} \int_{-\infty}^{\infty} S_p \exp(s g_p) \, \mathrm{d}\xi \, \mathrm{d}\kappa \tag{18}$$

with the phase of the source ray, $z \geqslant 0$, note the expression given in Eq. (11),

$$-t = g_p = \mathrm{i}\xi x + \mathrm{i}\kappa y - \eta z$$

and,

$$\bar{\psi}_{s,j} = \bar{\psi}_{0,j} + \lim_{z_0 \to 0} \left(\bar{\psi}_{Ps,j} + \sum_k \bar{\psi}_{S,ks,j} \right), \quad S_{s,j} = S_{0s,j} + S_P R^{PS,j} + \sum_k S_{S,k} R^{S,kS,j}, \quad j = x, y, z$$

yields finally,

$$\begin{aligned} S_{S_x} = {} & Q_x \left[(1 - R^{S_x S_x}) \frac{\xi\kappa(\eta - \zeta)}{\Delta_x} + R^{PS_x} \frac{\mathrm{i}\xi}{C^2 \Delta_x} - R^{S_y S_x} \right] + Q_y \left[(-1 + R^{S_x S_x}) - R^{PS_x} \frac{\mathrm{i}\kappa}{C^2 \Delta_y} + R^{S_y S_x} \frac{\xi\kappa(\eta - \zeta)}{\Delta_y} \right] \\ & + Q_z \left[-(1 + R^{S_x S_x}) \frac{\mathrm{i}\kappa}{\zeta} + R^{PS_x} + R^{S_y S_x} \frac{\mathrm{i}\xi}{\zeta} \right], \\ S_{S_y} = {} & Q_x \left[(1 - R^{S_y S_y}) + R^{PS_y} \frac{\mathrm{i}\xi}{C^2 \Delta_x} - R^{S_x S_y} \frac{\xi\kappa(\eta - \zeta)}{\Delta_x} \right] + Q_y \left[(-1 + R^{S_y S_y}) \frac{\xi\kappa(\eta - \zeta)}{\Delta_y} - R^{PS_y} \frac{\mathrm{i}\kappa}{C^2 \Delta_y} + R^{S_x S_y} \right] \\ & + Q_z \left[(1 + R^{S_y S_y}) \frac{\mathrm{i}\xi}{\zeta} + R^{PS_y} - R^{S_x S_y} \frac{\mathrm{i}\kappa}{\zeta} \right] \\ S_{S_z} = {} & 2 \left[Q_x \frac{\mathrm{i}\kappa}{\Delta_x} - Q_y \frac{\mathrm{i}\xi}{\Delta_y} \right] [\eta\zeta - (\xi^2 + \kappa^2)]. \end{aligned}$$

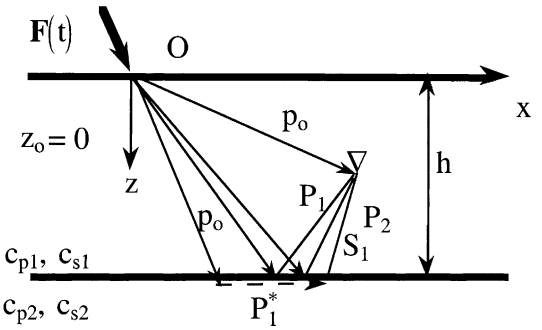

Fig. 4. P-waves emitted from a surface force and received at a buried receiver (where a local plastic source is expected). A plastic interlayer slip requires the limit of receiver depth taken to the layer thickness, Section 3.3.

$$\bar{\psi}_{s,j} = s^2 \overline{F}(s) \int_{-\infty}^{\infty} \int_{-\infty}^{\infty} S_{sj} \exp(s g_s)\, \mathrm{d}\xi\, \mathrm{d}\kappa, \quad j = x, y, z. \tag{19}$$

The common phase in the latter case is

$$-t = g_s = \mathrm{i}\xi x + \mathrm{i}\kappa y - \zeta z.$$

The nonvanishing reflection coefficients at the free surface of the plane wave potentials, R^{PP}, R^{PS_x}, R^{PS_y}, R^{S_xP}, R^{S_yP}, $R^{S_xS_x}$, $R^{S_yS_y}$, and $R^{S_xS_y} = R^{S_yS_x}$, $R^{S_zS_z} = 1$ to be inserted in Eqs. (18) and (19), are derived by Borejko (1996). Thus, the source ray integrals are given by Eqs. (16) and (17) after substitution of the above given emittance and phase functions. In Fig. 4, the p_0 "source ray" to a buried receiver is shown. Further, assuming a surface layer of thickness h, ray paths are indicated which illustrate an additional reflection of the p_0-ray at the interface to a fast bottom half space (transmission is not shown).

Since the acoustic signals emitted from any buried plastic source are received in an ultrasonic transducer at the surface, Eqs. (18) and (19) represent the proper complementary Green's function of the second kind. The Green's stress tensor at the location of the plastic source, i.e. at an interior point, is derived from Hooke's law which renders what is commonly called the stress receiver functions, note also the factors in Table 2 indicating time derivatives and use $\mathrm{div}\,\boldsymbol{\psi} = 0$.

3.3. Green's stress dyadic of the second kind received in an interlayer point

When a localized interlayer slip has to be considered as the plastic source, it becomes necessary to substitute the Green's stress dyadic received at this point into Eq. (6). A transducer in the receiving mode is commonly situated at the traction free surface, i.e. the solution of Section 3.2 applies, with a "receiver" situated within the surface layer, see again Fig. 4 for the (direct) p_0-source ray. The source ray, Eqs. (18) and

Table 2
Stress receiver functions at interior (plastic source) point, $\mu = \rho C^2$

3D-stress	Σ^{P}_{jk}/s^2	Σ^{Sx}_{jk}/s^2	Σ^{Sy}_{jk}/s^2	Σ^{Sz}_{jk}/s^2
σ_{xx}/μ	$\zeta^2 - \xi^2 + \kappa^2 - 2\eta^2$	0	$2\varepsilon(\mathrm{i}\xi)\zeta$	$-2\xi\kappa$
σ_{yy}/μ	$\zeta^2 + \xi^2 - \kappa^2 - 2\eta^2$	$-2\varepsilon(\mathrm{i}\kappa)\zeta$	0	$2\xi\kappa$
σ_{zz}/μ	$\zeta^2 + \xi^2 + \kappa^2$	$2\varepsilon(\mathrm{i}\kappa)\zeta$	$-2\varepsilon(\mathrm{i}\xi)\zeta$	0
σ_{xy}/μ	$-2\xi\kappa$	0	$2\varepsilon(\mathrm{i}\kappa)\zeta$	$-(\zeta^2 - \xi^2 + \kappa^2)$
σ_{yz}/μ	$-2\varepsilon(\mathrm{i}\kappa)\eta$	$\zeta^2 + \xi^2 + \kappa^2$	0	$2\varepsilon(\mathrm{i}\xi)\zeta$
σ_{zx}/μ	$-2\varepsilon(\mathrm{i}\xi)\eta$	$2\xi\kappa$	$-(\zeta^2 + \xi^2 - \kappa^2)$	0

Table 3
Stress receiver functions at interior (plastic source) point, $\mu = \rho C^2$

	σ_{xx}/μ		
$\overline{\Sigma}^{P}_{xx}/s^2$	$(1+R_{PP})(\zeta^2-\xi^2+\kappa^2-2\eta^2)-R_{PS_y}(2\mathrm{i}\xi\zeta)$	S_p	g_p
$\overline{\Sigma}^{Sx}_{xx}/s^2$	$R_{S_xP}(\zeta^2-\xi^2+\kappa^2-2\eta^2)-R_{S_xS_y}(2\mathrm{i}\xi\zeta)+R_{S_xS_z}(-2\xi\kappa)$	S_{s_x}	g_s
$\overline{\Sigma}^{Sy}_{xx}/s^2$	$(1-R_{S_yS_y})(2\mathrm{i}\xi\zeta)+R_{S_yP}(\zeta^2-\xi^2+\kappa^2-2\eta^2)+R_{S_yS_z}(-2\xi\kappa)$	S_{s_y}	g_s
$\overline{\Sigma}^{Sz}_{xx}/s^2$	$(1+R_{S_zS_z})(-2\xi\kappa)-R_{S_zS_y}(2\mathrm{i}\xi\zeta)$	S_{s_z}	g_s
	σ_{yy}/μ		
$\overline{\Sigma}^{P}_{yy}/s^2$	$(1+R_{PP})(\zeta^2+\xi^2-\kappa^2-2\eta^2)-R_{PS_x}(-2\mathrm{i}\kappa\zeta)$	S_p	g_p
$\overline{\Sigma}^{Sx}_{yy}/s^2$	$(1-R_{S_xS_x})(-2\mathrm{i}\kappa\zeta)+R_{S_xP}(\zeta^2+\xi^2-\kappa^2-2\eta^2)+R_{S_xS_z}(2\xi\kappa)$	S_{s_x}	g_s
$\overline{\Sigma}^{Sy}_{yy}/s^2$	$R_{S_yP}(\zeta^2+\xi^2-\kappa^2-2\eta^2)-R_{S_yS_x}(-2\mathrm{i}\kappa\zeta)+R_{S_yS_z}(2\xi\kappa)$	S_{s_y}	g_s
$\overline{\Sigma}^{Sz}_{yy}/s^2$	$(1+R_{S_zS_z})(2\xi\kappa)-R_{S_zS_x}(-2\mathrm{i}\kappa\zeta)$	S_{s_z}	g_s
	σ_{zz}/μ		
$\overline{\Sigma}^{P}_{zz}/s^2$	$(1+R_{PP})(\zeta^2+\xi^2+\kappa^2)-R_{PS_x}(2\mathrm{i}\kappa\zeta)-R_{PS_y}(-2\mathrm{i}\xi\zeta)$	S_p	g_p
$\overline{\Sigma}^{Sx}_{zz}/s^2$	$(1-R_{S_xS_x})(2\mathrm{i}\kappa\zeta)+R_{S_xP}(\zeta^2+\xi^2+\kappa^2)-R_{S_xS_y}(-2\mathrm{i}\xi\zeta)$	S_{s_x}	g_s
$\overline{\Sigma}^{Sy}_{zz}/s^2$	$(1-R_{S_yS_y})(-2\mathrm{i}\xi\zeta)+R_{S_yP}(\zeta^2+\xi^2+\kappa^2)-R_{S_yS_x}(-2\mathrm{i}\kappa\zeta)$	S_{s_y}	g_s
$\overline{\Sigma}^{Sz}_{zz}/s^2$	$-R_{S_zS_x}(2\mathrm{i}\kappa\zeta)-R_{S_zS_y}(-2\mathrm{i}\xi\zeta)$	S_{s_z}	g_s
	σ_{xy}/μ		
$\overline{\Sigma}^{P}_{xy}/s^2$	$(1+R_{PP})(-2\xi\kappa)-R_{PS_y}(2\mathrm{i}\kappa\zeta)$	S_p	g_p
$\overline{\Sigma}^{Sx}_{xy}/s^2$	$R_{S_xP}(-2\xi\kappa)-R_{S_xS_y}(2\mathrm{i}\kappa\zeta)+R_{S_xS_z}(-\zeta^2+\xi^2-\kappa^2)$	S_{s_x}	g_s
$\overline{\Sigma}^{Sy}_{xy}/s^2$	$(1-R_{S_yS_y})(2\mathrm{i}\kappa\zeta)+R_{S_yP}(-2\xi\kappa)+R_{S_yS_z}(-\zeta^2+\xi^2-\kappa^2)$	S_{s_y}	g_s
$\overline{\Sigma}^{Sz}_{xy}/s^2$	$(1+R_{S_zS_z})(-\zeta^2+\xi^2-\kappa^2)-R_{S_zS_y}(2\mathrm{i}\kappa\zeta)$	S_{s_z}	g_s
	σ_{yz}/μ		
$\overline{\Sigma}^{P}_{yz}/s^2$	$(1-R_{PP})(-2i\kappa\eta)+R_{PS_x}(\zeta^2+\xi^2+\kappa^2)-R_{PS_z}(2\mathrm{i}\xi\zeta)$	S_p	g_p
$\overline{\Sigma}^{Sx}_{yz}/s^2$	$(1+R_{S_xS_x})(\zeta^2+\xi^2+\kappa^2)-R_{S_xP}(-2\mathrm{i}\kappa\eta)-R_{S_xS_z}(2\mathrm{i}\xi\zeta)$	S_{s_x}	g_s
$\overline{\Sigma}^{Sy}_{yz}/s^2$	$-R_{S_yP}(-2\mathrm{i}\kappa\eta)+R_{S_yS_x}(\zeta^2+\xi^2+\kappa^2)-R_{S_yS_z}(2\mathrm{i}\xi\zeta)$	S_{s_y}	g_s
$\overline{\Sigma}^{Sz}_{yz}/s^2$	$(1-R_{S_zS_z})(2\mathrm{i}\xi\zeta)+R_{S_zS_x}(\zeta^2+\xi^2+\kappa^2)$	S_{s_z}	g_s
	σ_{zx}/μ		
$\overline{\Sigma}^{P}_{zx}/s^2$	$(1-R_{PP})(2\mathrm{i}\xi\eta)+R_{PS_x}(2\xi\kappa)+R_{PS_y}(-\zeta^2-\xi^2+\kappa^2)$	S_p	g_p
$\overline{\Sigma}^{Sx}_{zx}/s^2$	$(1+R_{S_xS_x})(2\xi\kappa)-R_{S_xP}(-2\mathrm{i}\xi\eta)+R_{S_xS_y}(-\zeta^2-\xi^2+\kappa^2)$	S_{s_x}	g_s
$\overline{\Sigma}^{Sy}_{zx}/s^2$	$(1+R_{S_yS_y})(-\zeta^2-\xi^2+\kappa^2)-R_{S_yP}(-2\mathrm{i}\xi\eta)+R_{S_yS_x}(2\xi\kappa)$	S_{s_y}	g_s
$\overline{\Sigma}^{Sz}_{zx}/s^2$	$R_{S_zS_x}(2\xi\kappa)+R_{S_zS_y}(-\zeta^2-\xi^2+\kappa^2)$	S_{s_z}	g_s

(19), (with the positive direction factor, $\varepsilon_z = 1$, already taken into account), and the rays reflected at the interface, their direction factor is -1,

$$\overline{\varphi_{pP}} = s^2\overline{F}(s)\int_{-\infty}^{\infty}\int_{-\infty}^{\infty} S_P R_{PP}\exp(sg_{pP})\,\mathrm{d}\xi\,\mathrm{d}\kappa; \tag{20}$$

$$\bar{\psi}_{pS,j} = s^2\overline{F}(s)\int_{-\infty}^{\infty}\int_{-\infty}^{\infty} S_P R_{PS,j}\exp(sg_{pS})\,\mathrm{d}\xi\,\mathrm{d}\kappa; \tag{21}$$

$$\overline{\varphi_{s,kP}} = s^2\overline{F}(s)\int_{-\infty}^{\infty}\int_{-\infty}^{\infty} S_{S,k} R_{S,kP}\exp(sg_{sP})\,\mathrm{d}\xi\,\mathrm{d}\kappa; \tag{22}$$

$$\bar{\psi}_{s,kS,j} = s^2\overline{F}(s)\int_{-\infty}^{\infty}\int_{-\infty}^{\infty} S_{S,k} R_{S,kS,j}\exp(sg_{sS})\,\mathrm{d}\xi\,\mathrm{d}\kappa \tag{23}$$

are superposed. The limit $z \to h$ of the depth of the buried receiver (the location of the plastic source) to the layer thickness is performed in the phase functions, Eqs. (18) and (19), see the right hand column of Table 3. The emittance functions in the P- and S_j potential functions of the coalescent ray are thus those of the source ray as derived in Eqs. (18) and (19) for the surface load, see Table 3 and note the lower case index referring to the downward incident ray.

The stress receiver functions follow from Hooke's law, see also Eq. (9), for a "receiver" sitting in the interface, and are tabulated, Table 3, in terms of the potential reflection coefficients at the interface of two dissimilar half spaces, for the latter see again Borejko (1996), and consider in the expressions given there a positive direction factor for the incident plane wave. Use has been made of $R_{PS_z} = R_{S_zP} = 0$.

As previously discussed requires a dipping interface the introduction of rotated coordinates for the consideration of classical reflection, the slowness are given by enforcing the invariance conditions, Eq. (12). More general configurations may be considered by using the information summarized in de Hoop (1995).

3.4. A numerical study of the Green's functions of the second kind

Inversion of the ray integrals by the Cagniard–de Hoop method has become a standard procedure, see e.g. Pao and Gajewski (1977), and, for details, the recent paper considering the three-dimensional wave propagation, Borejko et al. (2001). To indicate the sensitivity of the signal detection on the angular positioning of the transducer in receiving mode, we present in Figs. 5–10, Green's nondimensional

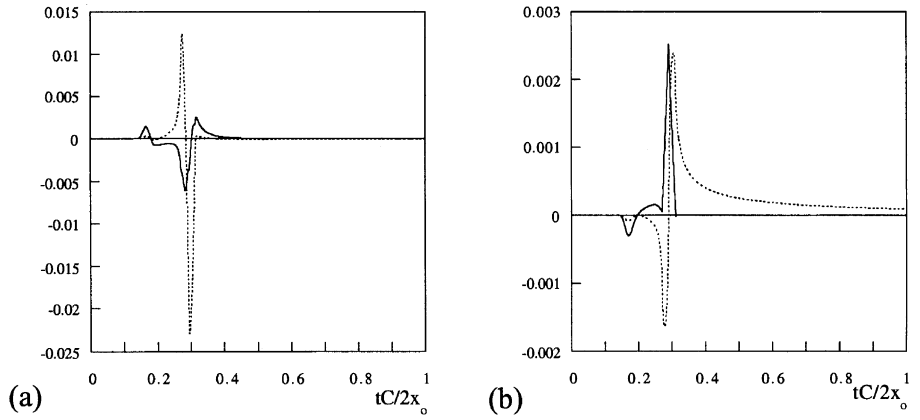

Fig. 5. Vertical outward (---) and horizontal (—) displacements of the surface point, (epicentral distance) $x = 0.25$, $y = z = 0$. (a) Vertical single surface force. (b) Vertical surface line load.

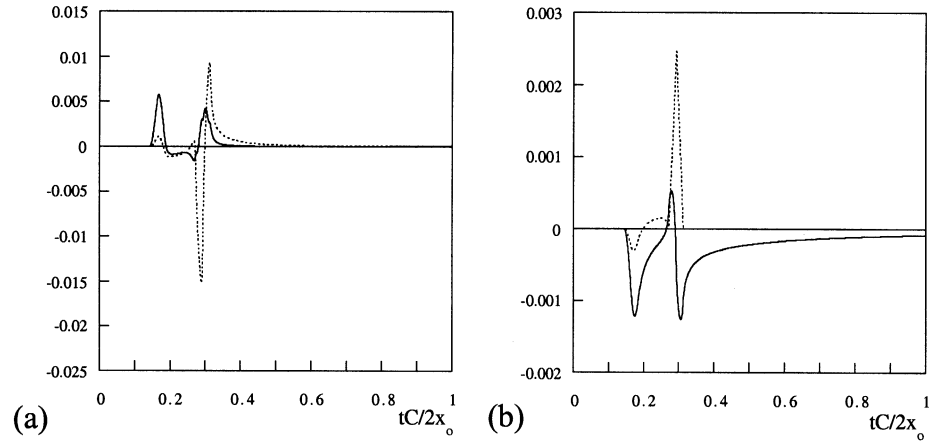

Fig. 6. Vertical outward (- - -) and horizontal (—) displacements of the surface point, (epicentral distance) $x = 0.25$, $y = z = 0$. (a) Horizontal single surface force. (b) Horizontal surface line load.

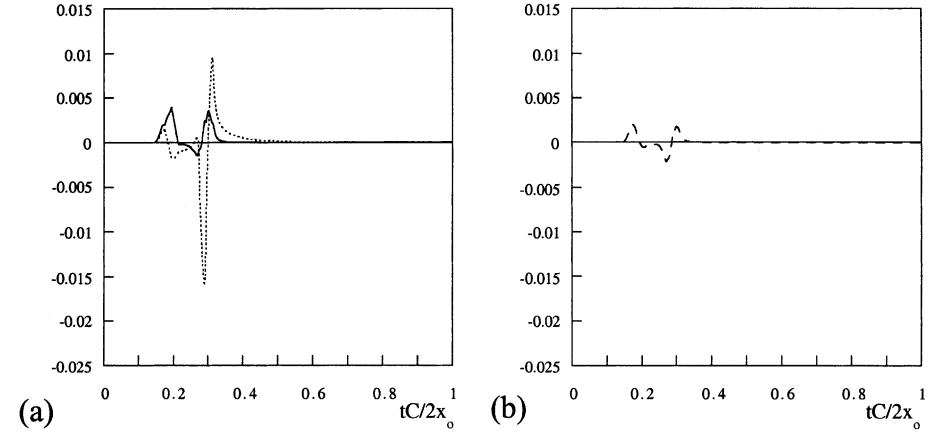

Fig. 7. (a) Vertical outward (- - -) and horizontal (—) displacements of the surface point, $x = 0.2165$, $y = 0.1250$. (b) Lateral horizontal displacement (in y-direction). Horizontal single surface force in x-direction.

displacement components, horizontally, u_x and (laterally) u_y, and, vertically outward, $-u_z$, produced by a symmetric triangular pulse of nondimensional and short duration 0.04 and nondimensional tip value 0.02, (hence, rise-time $\Delta = 0.02$ and nondimensional peak value Δ), applied at the surface, which are "received" at a surface point of a half space (body wave speeds, $c_L = \sqrt{3}$, $c_S = 1$, and uniform density $\rho = 1$) in the nondimensional epicentral radial distance $r = 0.25$. Further, the impulsive force is stepwise rotated from the vertical over $\pi/4$ the inclined to the horizontal direction. For comparison sake with the point force solution, the two-dimensional response to a line load of same time signature is shown in the Figs. 5(b) and 6(b).

Taking into account the demonstrated sensitivity of the angular positioning of the transducer in receiving mode (when parallel to the oblique single force), time convolution (of the stresses due to the oblique force) with a given plastic strain tensor, Eq. (6), thus renders dramatically changed signals.

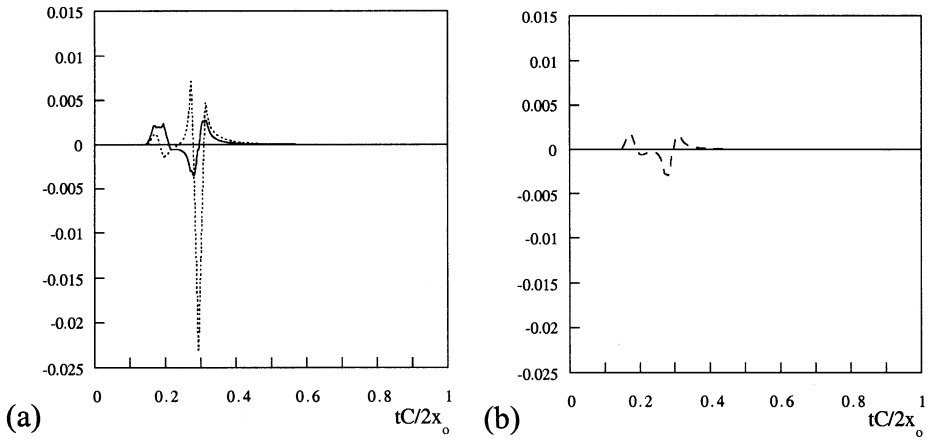

Fig. 8. (a) Vertical outward (- - -) and horizontal (—) displacements of the surface point, $x = 0.2165$, $y = 0.1250$. (b) Lateral horizontal displacement (in y-direction). Oblique single surface force, positively rotated $\pi/4$ in the x–z plane.

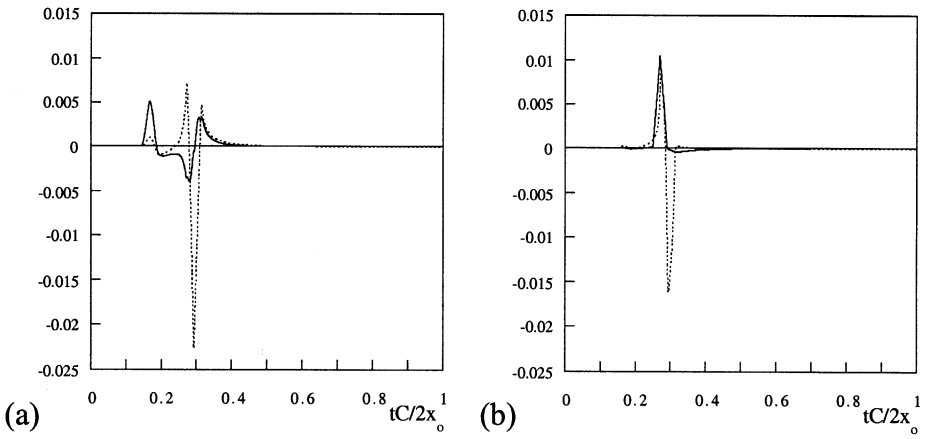

Fig. 9. Vertical outward (- - -) and horizontal (—) displacements at two surface points. Oblique single surface force, positively rotated $\pi/4$ in the x–z plane. (a) Receiver at (epicentral distance) $x = 0.25$, $y = z = 0$. (b) Receiver at (lateral epicentral distance) $x = 0$, $y = 0.25$.

4. Conclusions

Identification of waves from plastic sources is of great importance in monitoring the safety of ductile structures eventually under the action of dynamic overload. To locate the plastic source emitting the acoustic signal by triangulation needs at least three separately placed transducers, see Pao (1978). Since the transducer in receiving mode is located at the free surface we select the complementary Green's stress dyadic of the second kind for the convolution with the localized plastic source. Superiority of Eq. (6) over Eq. (5) or other classical convolution integrals, like the Mura–Willis integral, should be emphasized. All the characteristic features of the wave guide are contained in the Green's function, these facts are demonstrated within the paper for thin rods, for plates and for a layered half-space. In the latter case the Green's functions are expanded into plane waves. The plastic interlayer slip, Section 3.3, is an important special case and is considered by properly changing the stress receiver functions in the Green's stress dyadic, see

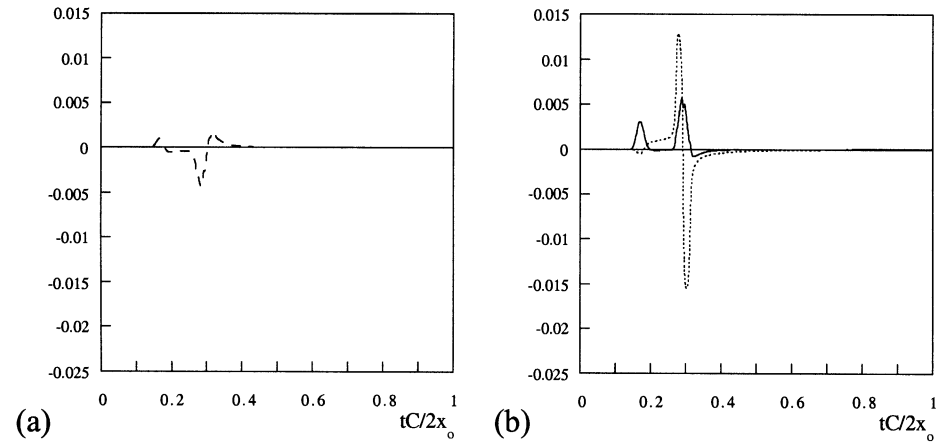

Fig. 10. Oblique single surface force, positively rotated $\pi/4$ in the x–z plane. (a) Receiver at (lateral epicentral distance) $x = 0$, $y = 0.25$, lateral horizontal displacement (in y-direction). (b) Receiver at (epicentral distance) $x = -0.25$, $y = z = 0$. Vertical outward (- - -) and horizontal (—) displacements. Inspect Fig. 9 (a) to see the "unsymmetry".

Eqs. (18) and (19) for superposition and Table 3. Since the influence functions of stresses enter the generalized dynamic Maysel's formula, receiver functions become the additional factors in the ray integrals together with higher powers of the Laplace transform variable s. For cylindrical waves, these functions are tabulated in Ziegler and Irschik (2000), for spherical waves see Tables 2 and 3. All necessary transformations of the Cagniard-de Hoop inversion technique are performed symbolically, for details see Pao and Gajewski (1977), Borejko and Ziegler (2002). Thus, the response of a single plastic source is fully accounted for by varying the receiver coordinates in the Green's stress dyadic. Eventually contributions from non-vanishing initial conditions arise, see Eq. (6), which are not further discussed in the paper. The matrix notation introduced in the IUTAM selected landmark paper by Pao and Gajewski (1977), is a starting point for such an enterprise. Deconvolution is not within the scope of this paper.

Acknowledgements

The numerical results contained in the Figs. 5–10 have been derived by Piotr Borejko in extension of the research contract, granted by the Austrian Research Foundation FWF, during his tenure as a Senior Scientist at the Tech. University of Vienna. His computational efforts are gratefully acknowledged.

References

Achenbach, J.D., 1973. Wave Propagation in Elastic Solids. Elsevier Science, Amsterdam.

Achenbach, J.D., 1987. Flaw characterization by ultrasonic scattering methods. In: Achenbach, J.D., Rajapakse, Y. (Eds.), Proceedings ONR Symposium on Solid Mechanics Research for Quantitative Nondestructive Evaluation QNDE. Martinus Nijhoff Publ, Dordrecht, pp. 67–81.

Achenbach, J.D., 2000. Calculation of wave fields using elastodynamic reciprocity. Int. J. Solids Struct. 37, 7043–7053.

Achenbach, J.D., Gautesen, A.K., McMaken, H., 1982. Ray Methods for Waves in Elastic Solids—with applications to scattering by cracks. Pitman, Boston.

Achenbach, J.D., Xu, Y., 1999. Wave motion in an elastic layer generated by a time-harmonic point load of arbitrary direction. J. Acoust. Soc. Am. 106, 83–90.

Aki, K., Richards, P., 1980. Quantitative Seismology, vol. 1. W.H. Freeman, San Francisco.

Borejko, P., 1996. Reflection and transmission coefficients for three-dimensional plane waves. Wave Motion 24, 371–393.
Borejko, P., Chen, C.F., Pao, Y.H., 2001. Application of the method of generalized rays to acoustic waves in a liquid wedge over elastic bottom. J. Comput. Acoust. 9, 41–68.
Borejko, P., Ziegler, F., 1998. Influence of the dipping angle on seismic response spectra. In: Proceedings Big Cities World Conference on Natural Disaster Mitigation, Cairo University Publishing and Printing Center 1997/2229, Cairo, pp. 73–92.
Borejko, P., Ziegler, F., 2002. Pulsed asymmetric point force loading of a layered half-space. In: Guran, A., Boström, A.A., Leroy, O. (Eds.), Acoustic Interactions with Submerged Elastic Structures. Part 4: NonDestructive Testing, Acoustic Wave Propagation and Scattering. World Scientific, Singapore, Ch. 9.
Ceranoglu, A.N., Pao, Y.-H., 1981. Propagation of elastic pulses and acoustic emission in a plate. Part I. Theory, Part II. Epicentral response, Part III. General responses. ASME J. Appl. Mech. 48, 125–147.
de Hoop, A.T., 1995. Handbook of Radiation and Scattering of Waves. Academic Press, London.
Eringen, A.C., Suhubi, E.S., 1975. Elastodynamics. II. Academic Press, New York.
Fotiu, P.A., Irschik, H., Ziegler, F., 1991. Micromechanical foundations of dynamic plasticity with applications to damaging structures. In: Brüller, O. et al. (Eds.), Advances in Continuum Mechanics. Springer, Berlin, pp. 338–349.
Fotiu, P.A., Ziegler, F., 1996. The propagation of spherical waves in rate-sensitive elastic-plastic materials. Int. J. Solids Struct. 33, 811–833.
Guo, D., Mal, A.K., Ono, K., 1996. Wave theory of acoustic emission in composite laminates. J. Acoust. Emission 14, S19–S46.
Irschik, H., Fotiu, P.A., Ziegler, F., 1993. Extension of Maysel's formula to the dynamic eigenstrain problem. J. Mech. Behav. Mater. 5, 59–66.
Irschik, H., Ziegler, F., 1990. Uniaxial dissipative elastic waves due to high velocity impact. In: Achenbach, J.D., Datta, S.K., Rajapakse, Y.S. (Eds.), Proceedings IUTAM-Symp. on Elastic Wave Propagation and Ultrasonic Nondestructive Evaluation. North-Holland, Amsterdam, pp. 333–338.
Irschik, H., Ziegler, F., 1995. Dynamic processes in structural thermo-viscoplasticity. AMR 48, 301–316.
Mal, A.K., 2001. Elastic waves from localized sources in composite laminates. In: Sotiropoulos, D.A. (Ed.), Proceedings IUTAM Symposium on Mechanical Waves for Composite Structures Characterization. Kluwer Academic Publ, Dordrecht, pp. 1–23.
Ohira, T., Pao, Y.-H., 1987. Acoustic emission source characterization of microcracking in A533B steel. In: Achenbach, J.D., Rajapakse, Y. (Eds.), Solid Mechanics Research for Quantitative NonDestructive Evaluation. Martinus Nijhoff Publ, Dordrecht, pp. 411–423.
Pao, Y.-H., 1978. Theory of acoustic emission. In: Pao, Y.-H. (Ed.), Elastic Waves and NonDestructive Testing of Materials, AMD-Vol. 29. ASME, New York, pp. 107–128.
Pao, Y.-H., Gajewski, R.R., 1977. The generalized ray theory and transient responses of layered elastic solids. Phys. Acoust. 13, 183–265.
Pao, Y.-H., Sachse, W., Fukuoka, H., 1984. Acoustoelasticity and ultrasonic measurements of residual stresses. Phys. Acoust. 17, 62–143.
Sachse, W., 1987. Applications of quantitative acoustic emission methods: dynamic fracture, materials and transducer characterization. In: Achenbach, J.D., Rajapakse, Y. (Eds.), Proceedings of the ONR Symposium on Solid Mechanics Research for Quantitative Nondestructive Evaluation, QNDE. Martinus Nijhoff Publ, Dordrecht, pp. 41–64.
Simmons, J.A., Wadley, H.N.G., 1984. Theory of acoustic emission from inhomogeneous inclusions. In: Johnson, G.C. (Ed.), Wave Propagation in Homogeneous Media and Ultrasonic Nondestructive Evaluation, AMD-Vol. 62. ASME, New York, pp. 51–59.
Ziegler, F., 1998. Mechanics of Solids and Fluids, Corr. repr. of 2nd ed. Springer, New York.
Ziegler, F., Borejko, P., 2000. The method of generalized ray-revisited. The Chinese J. Mech. 16, 45–52, Erratum: 125–126.
Ziegler, F., Irschik, H., 2000. Elastic–plastic waves by superposition in the elastic background. ZAMM 80 (Suppl. 1), S109–S112.